Antonie van Leeuwenhoek **59**: 27–34, 1991.

Fine-structural and chemical analyses on inner and outer sheath of the cyanobacterium *Gloeothece* sp. PCC 6909

B. Tease,[1] U.J. Jürgens,[1] J.R. Golecki, [1] U.-R. Heinrich, [2] R. Rippka[3] & J. Weckesser[1]
[1] *Institut für Biologie II, Mikrobiologie, Schänzlestr. 1;* [2] *Institut für Biophysik und Strahlenbiologie, der Albert-Ludwigs-Universität, Albertstr. 23, D-7800 Freiburg i. Br., Germany;* [3] *Institut Pasteur, 28, Rue du Dr. Roux, 75724 Paris Cedex 15, France*

Received 19 April 1990; accepted 15 October 1990

Key words: cyanobacteria, *Gloeothece, sheath,* sulfated polysaccharide, electron spectroscopic imaging

Abstract

Cells of the unicellular cyanobacterium *Gloeothece* sp. PCC 6909 are surrounded by an inner (enclosing 1–2 cells) and an outer (enclosing cell groups) sheath. Using conventional Epon-embedding in combination with ruthenium-red staining, the inner and outer sheaths appeared similar and displayed multiple bands of electron-dense subunits. However, embedding in Nanoplast resin to avoid shrinkage led to the detection of two distinct zones (inner and outer zone) each with several distinct layers. The zone delimited by the electron-dense thick inner sheath layer, and the zone enclosed by the thin electron-dense outer sheath layer, are composed of a homogeneous material of little electron-contrast. Whereas the outer zone appears to be of even contrast, the inner zone is characterized by a distinct electron-transparent layer. Element distribution analysis revealed that the electron-transparent layer contained relatively large amounts of sulfur, carbon, and oxygen but only little nitrogen.

Inner and outer sheath fractions were isolated by differential mechanical cell breakage and centrifugation. The outer sheath fraction was less hydrated than the inner one. The two fractions differed little in their contents of uronic acids, carbohydrate and protein, although the outer sheath fraction contained less sulfate. A soluble polysaccharide with a chemical composition similar to that of inner and outer sheath fractions was also obtained from the culture supernatant.

Introduction

Cells of the unicellular cyanobacterium *Gloeothece* sp. produce a sheath. The nascent sheath is initially formed adjacent to the outer membrane and, after cell division, detaches and expands to accomodate the growing cell population that it encloses. Individual cells produce new sheath layers, resulting in several ensheathed clusters of 1 to 4 cells within larger aggregates of 4 to 16 cells (Kallas et al. 1983; Rippka et al. 1979; Stanier & Cohen-Bazire 1977). Consequently, the cells are surrounded by inner (surrounding 1–2 cells) and outermost (surrounding cell groups) sheath layers with zones of varying thickness between them.

The sheath of *Gloeothece* sp. is composed of complex heteropolysaccharides which contain sulfate groups (Tease & Walker 1987; Weckesser et al. 1987), as was recently also described for the bioflocculant from *Phormidium* sp. J-1 (Bar-Or & Shilo 1987). However, the previous analyses on *Gloeothece* sp. were performed on total sheath envelopes. We now found these envelopes to be composed of several distinct layers. The fine structure,

isolation and chemical composition, and the element distribution of the various sheath fractions are described here.

Materials and methods

Strain and cultivation

The organism under study was *Gloeothece* sp. PCC 6909 from the Pasteur Culture Collection, Institut Pasteur, Paris, France. Cells were grown photoautotrophically in BG-11 medium (Allen & Stanier 1969), without $NaNO_3$, at 27° C in a 12 l fermentor, aerated with prefiltered compressed air. Continuous illumination was provided from a bank of white fluorescent lamps (1,000–2,000 lx). Cells were harvested 8 to 12 days after inoculation.

Isolation of sheath fractions

Cells from 10 l culture medium were concentrated, after settling overnight and syphoning of the medium, by centrifugation at 1,000 × *g* for 10 min. A portion of this cell pellet was mixed with glass beads (0.17–0.18 mm in diameter, Braun, Melsungen, Germany; cell to glass bead ratio 1 : 3, v/v), in distilled water and vibrated at full speed in a vibrogen shaker, type Vi2 (Bühler, Tübingen, Germany) at 4° C. The outer sheath was liberated after 5 min without inducing cell breakage, as evidenced by the absence of pigment release. Removal of inner sheath required 40 min treatment due to its greater mechanical stability. Inner and outer sheath fractions differed in appearance and physical properties. The outer sheath was more compressed (less hydrated) and opaque compared to the more hydrated, transparent inner sheath fraction. A soluble sheath polysaccharide (obtained by concentration, dialysis and lyophilization) was identified in the culture supernatant.

Fractured sheath material was collected after filtering the cell and glass bead slurry through a glass filter (GF-1, Schott, Mainz, Germany). Fractured sheath material was separated from intact cells by sequential centrifugation for 5 to 10 min at 250 × *g*, 1,000 × *g* and 38,000 × *g*. The material in the final pellet, composed primarily of single ensheathed cells, was treated an additional 40 min to liberate the mechanically more resistant inner sheath. The inner sheath was isolated by differential centrifugation as above.

Lysozyme and sodium lauryl sarkosin treatment

The sheath fractions were treated with lysozyme (1 mg/5 mg sheath material in 20 mM ammonium acetate buffer, pH 7.0) to insure removal of any cell wall (peptidoglycan) contamination. Samples were stirred for 7 h at 37° C and continued for 10 h at 6° C. After 3 rinses with distilled water, each followed by centrifugation at 38,000 × *g* for 10 min, the sheath fractions were treated in 2% sodium lauryl sarkosin for 24 h at 25° C. The sheath fractions were rinsed 5 times with 30 ml of distilled water, each followed by centrifugation at 38,000 × *g* for 10 min.

Soluble polysaccharide isolation

Approximately 4 l of culture supernatant were concentrated by rotary evaporation at 35° C to a final volume of 250 ml. Following ultracentrifugation (120,000 × *g*, 4° C, 0.5 h) and lyophilization, salts were removed by dialysis against distilled water. The remaining non-dialyzable material was lyophilized.

Analytical procedures

A microversion of the turbidometric-barium chloride assay for sulfate in aqueous solutions (American Public Health Association 1980) was developed to assay for sulfate in sheath fractions. About 200 to 300 μg of lyophilized sheath were hydrolyzed in 0.5 ml of 1 M HCl at 100° C for 24 h. The liquid was evaporated under a stream of nitrogen gas at 30° C prior to the addition of 1.0 ml of water and 0.05 ml of the conditioning reagent (3.0 ml water, 0.3 ml concentrated HCl, 1.0 ml 95% isopropa-

nol, 0.5 ml glycerol and 0.75 g NaCl). After measuring the absorbance at 420 nm, approximately 25 mg of $BaCl_2$ were added. Samples were vortexed for 1 min and the absorbance (420 nm) was measured again after 4 min for determination of increasing optical density due to $BaSO_4$ precipitation. The sulfate content was estimated as the difference of the maximal absorptions before and after addition of $BaCl_2$. For infrared spectroscopy, a KBr pellet (using 1 mg of lyophilized sheath material) was prepared and an infrared spectrum taken using a Perkin-Elmer fourier-transform infrared spectrophotometer, model 1500. Amino acids and amino sugars were determined after hydrolysis (4 M HCl, 105° C, 18 h) in an automatic amino acid analyzer, model LC 6001 (Biotronik, München, Germany). Uronic acids were determined by the m-phenylphenol colorimetric assay (Blumenkrantz & Asboe-Hansen 1973). Neutral and uronic acid sugars were determined after hydrolysis (1 M HCl, 100° C, 10 h) and identified by combined gas-liquid chromatography/mass spectrometry as their alditol acetates (Sawardeker et al. 1965). Prior to polymer hydrolysis, the carboxylate groups of the uronic acids were methylated by stirring lyophilized sheath material in 'magic methanol' (dry methanol/concentrated HCl/trichloromethane = 10 : 1 : 1, v/v/v) for 24 h at 25° C and subsequently reduced to the corresponding alcohol with sodium borohydride (2 mg/mg dry weight of sheath: 6° C, 24 h). Deuterated hexoses were interpreted as uronic acids by mass spectrometry. The ratio of peak heights (m/e's of 217 to 217 plus 218) were used to determine the proportions of each hexuronic acid present (Fazio et al. 1982). A Varian aerograph, model 1440 gas-liquid chromatograph equipped with a 150 cm × 3 mm glass column containing 3% ECNSS-M on Gas Chrom-Q (100–200 mesh) was used for the analysis of neutral sugars as their alditol acetate derivatives (program rate: 2° C/min, 150 to 180° C). Mass spectrometry was performed (using chemical ionization) with a Finnigan automatic GC-MS system model MAT 1020 B.

Electron microscopy

Cells, before and after outer sheath removal, were fixed with 1% OsO_4 in cacodylate buffer or with 2% glutaraldehyde followed by 1% OsO_4, dehydrated by ethanol (70 to 100%) and embedded in Epon according to Luft (1961). A treatment with ruthenium red (Luft 1964) was performed to demonstrate the presence of acidic polysaccharides. Alternatively, cells were embedded in Nanoplast resin (Bachhuber & Frösch 1983) without a preceeding fixation step and dehydration by alcohol. For conventional transmission electron microscopy ultrathin sections were stained with uranyl acetate and lead citrate before examination in a Philips EM 400 at 80 kV (Golecki 1977). From the same material ultrathin sections without any staining were examined for chemical analysis with electron microscopic imaging in a Zeiss EM 902 equipped with an electron energy spectrometer (Bauer 1988). Element distribution analysis and elemental mapping were performed by spectroscopic determination of the element-specific energy losses of inelastically scattered electrons. Elemental maps were produced by computer-assisted photographic image processing (Bauer 1988). The presence of specific elements is indicated by light and their absence by dark appearance.

Results

Fine-structure of the sheath layers

Conventional Epon-embedding and ruthenium-red staining of ultrathin sections of *Gloeothece* sp. PCC 6909 revealed multiple bands of electron-dense material throughout the sheath envelopes. As a result of dehydration by ethanol, necessary for embedding with Epon, the bands were mainly composed of electron-dense subunits (mean diameter of 40 nm, center to center spacing of 25 nm) (Fig. 1), except for certain areas in the outer sheath zones in which the bands were continuous. In contrast, ultrathin sections of cells embedded in Nanoplast resin did not show this artifact, attributable to shrinkage (Figs 2 and 3). Here the sheath lacked

the multiple banded fine-structure seen in the Epon-embedded sections, rather it displayed two broad zones of homogeneous material, one within the boundaries of the thick electron-dense inner sheath layer (IL) and one within the boundaries of the thinner electron-dense outer sheath layer (OL). The inner and outer zones, each, may contain more than one additional layers with varying thickness and electron-contrast. A characteristic layer (IL^+, ⇨ in Figs 2 and 3) which appeared partly electron-transparent or weakly stained, was observed in the inner sheath zone.

Element distribution in the sheath

The element distribution within the sheath substructures was revealed by element spectroscopic imaging. An overview of the multiple sheath layers of a cell aggregate is presented in Fig. 4a as bright field image. The marked area indicates the section analyzed for elemental mapping with electron spectroscopic imaging. A layer (IL^+, ⇨ also in Figs 2a, 3, 4b–d) seen dark in this bright field image corresponds to the characteristic layer of low contrast in Figs 2a and 3. It is characterized by a higher content of sulfur (Fig. 4b), carbon (Fig. 4c) and oxygen (Fig. 4d) and a lower content of nitrogen (Fig. 4e) in comparison to the surrounding sheath regions. However, as indicated by the dark banding pattern, the carbon content is very low in two layers of the outer sheath, whereas the inner sheath (Fig. 4c) seems to be rich in carbon.

Chemical composition of inner and outer sheath fractions

The chemical compositions of the inner and outer sheath fractions (after lysozyme/sodium lauryl sarkosin treatment) were very similar with respect to their contents of rhamnose, 2-*O*-methyl-xylose, xylose, mannose, galactose, glucose, as well as mannuronic, glucuronic and galacturonic acids. Protein and sulfate were detected in both fractions (Table 1). The infrared spectrum showed a strong absorption band at 1,610 cm^{-1} (data not shown) characteristic of carboxylate ions (Schleifer et al. 1982). Furthermore, a substantial increase in the amounts of neutral sugars was observed after reduction of the carboxyl groups of uronic acids with sodium borohydride prior to hydrolysis (Table 1), compared to the amounts obtained without the latter reduction step. Thus, the sodium borohydride treatment permitted a more efficient hydrolysis of sheath material, which indicates that the unsubstituted carboxyl groups of uronic acids exert a protective effect against acid hydrolysis of the glycosidic linkages. The carboxyl groups of the uronic acids were at least partially unsubstituted. Amino sugars were absent from the sheath material as revealed by amino acid analysis.

Quantitative differences were found between the outer and inner sheath fractions with respect to their contents of uronic acids, protein and sulfate. Based on colorimetric analysis, the outer sheath fraction contained 45% more total uronic acids than the inner sheath fraction (Table 1). The respective molar ratios determined by combined gas-

→

Fig. 1. Ultrathin section of *Gloeothece* sp. PCC 6909 after ruthenium-red staining and embedding in Epon. The polysaccharide-positive sheath material characterized by regular arranged electron-dense subunits of 40 nm in diameter is indicated by black arrow heads (▶). Inner (IL, ⇨) and outer (OL, ⇨) layers are surrounding 1–2 cells or cell groups, respectively. Bar represents 5 μm.

Fig. 2. Ultrathin section of *Gloeothece* sp. PCC 6909 after Nanoplast embedding without fixation. (a) The cell aggregate is surrounded by the inner and outermost sheath layers surrounding the inner (IZ) and outer (OZ) zones, respectively. No shrinkage is visible. The arrows mark the characteristic layer (IL^+ ⇨), which was demonstrated by Electron Spectroscopic Imaging to be of different element concentration (see Fig. 4). Bar represents 5 μm. (b) Detail of cell aggregate surrounded by several sheath layers. More than one layer (indicated by IL and OL, respectively) can be seen within inner and outer zones. Bars represent 5 μm (a) and 1 μm (b).

Fig. 3. Section of the inner sheath zone after Nanoplast embedding without fixation. Note among this zone the characteristic layer of lower contrast (IL^+ ⇨). Not also the fine structure (inset) of the cell wall (CW, 30–40 nm thick) with outer membrane (OM, 8–9 nm thick) and peptidoglycan (PG, 8–14 nm thick) and of the cytoplasmic membrane (CM, 7–8 nm thick). Bar represents 1 μm (in the inset 100 nm).

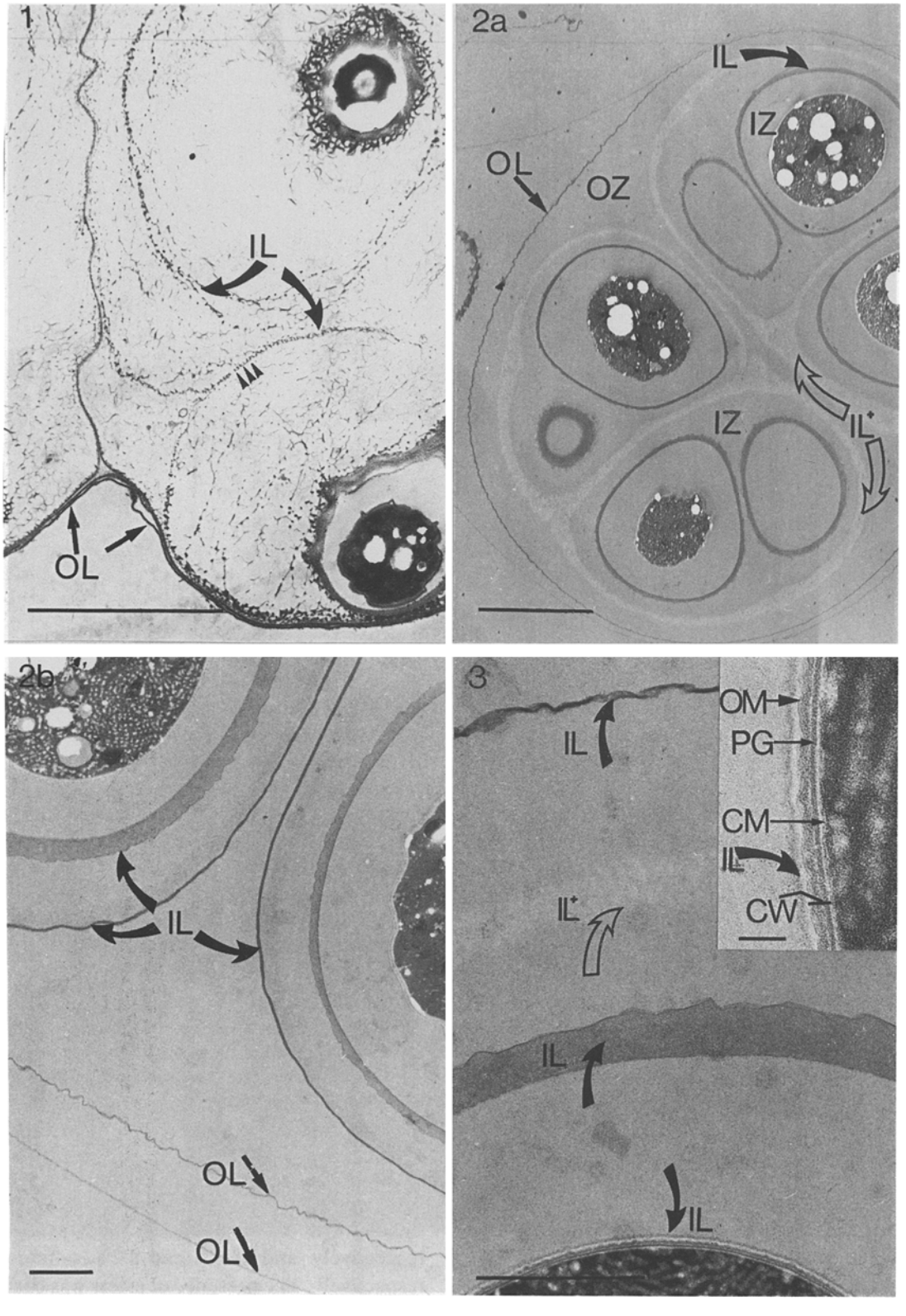

Figs 1–3.

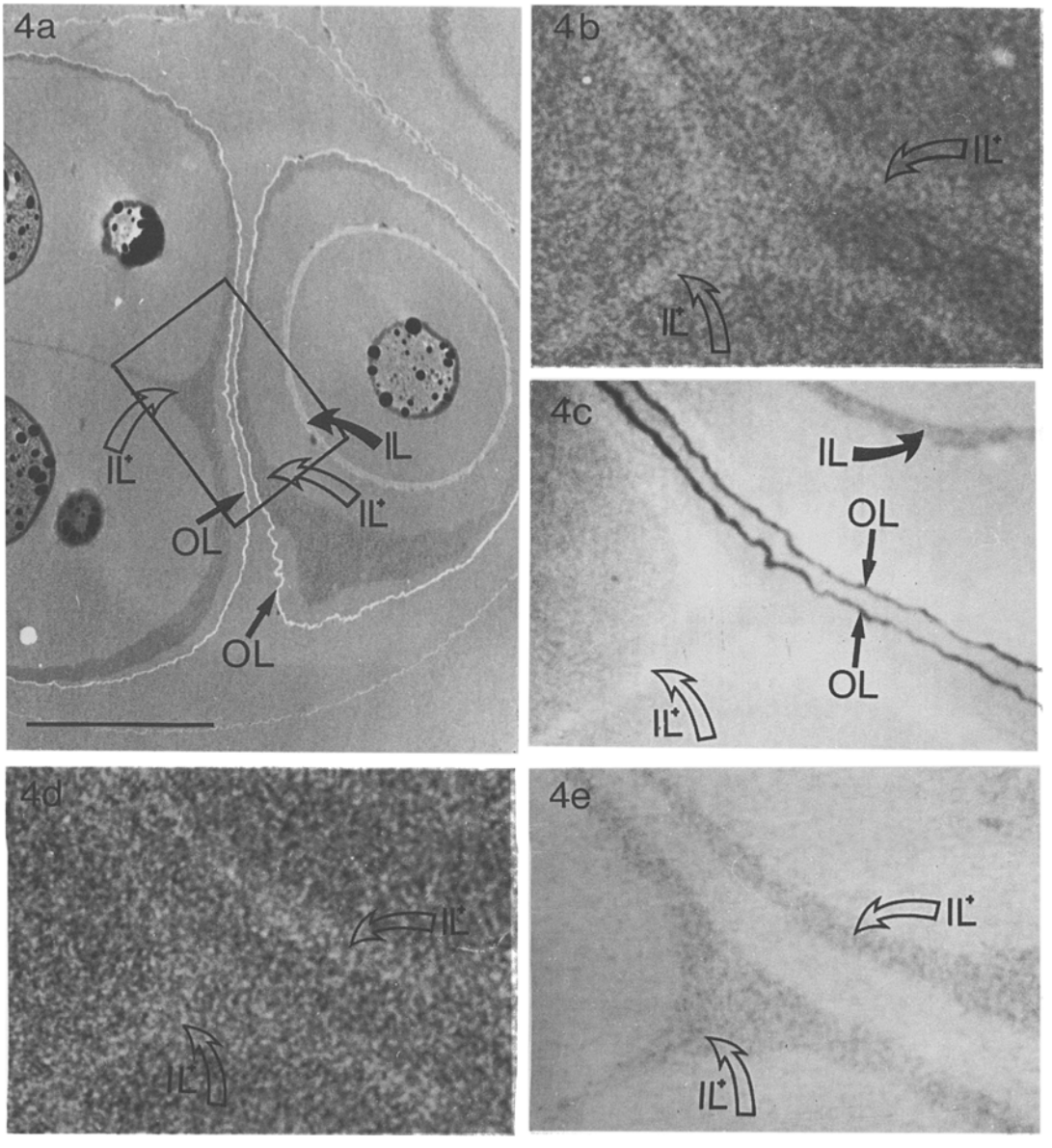

Fig. 4. Elemental mapping of *Gloeothece* sp. PCC 6909 by electron spectroscopic imaging. Light areas indicate the presence of elements. The layer, marked by the arrow (⇀) in each Figure, corresponds to an area equivalent to the characteristic layer of lower contrast shown in Figs 2 and 3. (a) Overview of a cell aggregate as brightfield image (for increasing the contrast by filtering out the inelastically scattered electrons [Bauer 1988]). The boxed area indicates the field analysed for different elements, the results of which are shown in Figs 4b–e. (b) Sulfur net distribution ($\Delta E = 185$ eV – $\Delta E = 155$ eV). (c) Carbon net distribution ($\Delta E = 304$ eV – $\Delta E = 264$ eV). Dark areas indicate absence of carbon. (d) Oxygen net distribution ($\Delta E = 552$ eV – $\Delta E = 512$ eV). (e) Nitrogen net distribution ($\Delta E = 421$ eV – $\Delta E = 381$ eV).

liquid chromatography/mass spectrometry for mannuronic, glucuronic and galacturonic acids for inner and outer sheath fractions were 1.0 : 1.9 : 4.0 and 1.0 : 3.4 : 3.6, respectively. The inner and outer sheath fractions contained 2.4% and 4.4% protein, respectively, and 18.6% and 8.2% sulfate esters, respectively. The presence of esters was confirmed by IR-spectroscopy (data not shown), which

Table 1. Chemical analyses (mg/100 mg dry weight) of the inner and outer sheath and soluble polysaccharide fractions obtained from the culture supernatant.

Compound	Inner sheath	Outer sheath	Soluble polysaccharide
Rhamnose	2.6 (2.3)	2.9 (0.8)	3.0 (1.7)
2-*O*-Methyl-D-xylose	2.2 (1.0)	3.0 (0.5)	1.5 (0.7)
Xylose	1.5 (1.1)	1.3 (0.4)	1.7 (0.8)
Mannose	3.7 (3.7)	3.7 (1.4)	5.3 (2.9)
Galactose	7.9 (4.5)	6.4 (1.5)	8.2 (4.0)
Glucose	6.4 (5.4)	7.4 (2.3)	9.8 (5.6)
Total uronic acids	2.9	4.2	5.0
Sulfate	18.6	8.2	13.8
Protein	2.4	4.4	6.2

Values in parentheses represent neutral sugar content prior to reduction of carboxyl groups of uronic acids with sodium borohydride.

showed a strong absorption band at 1,240 cm^{-1}. Absorption at 850 cm^{-1} may indicate the presence of sulfate esters in an axial conformation (Turvey 1965). Both sheath fractions were free of cell wall components as evidenced by the absence of muramic acid and diaminopimelic acid. The chemical composition of the soluble polysaccharide, obtained from the culture supernatant, is given in Table 1.

Discussion

Ultrathin sections of *Gloeothece* sp. PCC 6909 cells, prepared without fixation and embedding in Nanoplast resin, did not display the shrinkage of sheath that results from the conventional ethanol dehydration and Epon embedding procedures. The highly hydrated intermediate sheath layers and zones appeared well preserved and seemed to be similar in proportion to those viewed in the light microscope. This holds true also for both the inner (surrounding single cells) and outer (surrounding cell groups) sheath layers. The Nanoplast embedding does not include organic solvents for dehydration (loss and dislocation of extracted sheath substances are thus avoided). For this reason, the method is especially suitable for element distribution analysis with electron spectroscopic imaging in this study.

The ease with which the outer sheath of *Gloeothece* sp. PCC 6909 was broken, facilitated its isolation without cell breakage. The chemical compositions between the inner and outer sheath fractions were similar, although a higher content of sulfate esters was determined for the inner sheath by both analytical-chemical methods and by fine-structural element distribution analysis. The soluble polysaccharide fraction, obtained from the culture supernatant had a similar chemical composition compared to the isolated sheath. It cannot be excluded that this fraction or part of it was released from lysed cells during growth. The higher transparency of the inner sheath material of *Gloeothece* sp. PCC 6909 compared to the opaque, less hydrophilic outer sheath material may be attributed to its higher content of sulfate esters. This higher sulfate content reminds on the highly sulfated algal polysaccharides (Percival 1979). Sulfate or other acidic substituents like phosphate groups have a high capacity of collecting ions. Also, they will certainly contribute to protect the cell against desiccation by increasing the wetability of polysaccharides (Rees 1972). Uronic acid sulfate esters have been found in the heteropolysaccharides of the cell envelope of *Halococcus morrhuae* (Schleifer et al. 1982) and in the surface glycoprotein of *Halobacterium halobium* (König 1987). It has to be studied whether – like in these cases – sulfate is substituting the uronic acids found in the sheath of *Gloeothece* sp. PCC 6909. Negatively charged groups in the cell envelope seem to be indispensible for the viability of the

cell, as documented by the presence of polymers such as teichoic acids, acidic capsule polysaccharides or lipopolysaccharide in many other bacteria (Beveridge 1981).

Acknowledgements

The authors thank D. Borowiak for mass spectra and B. Raffelsberger for infrared spectra. B. Tease had a fellowship from the Deutsche Akademische Austauschdienst (DAAD).

References

Allen MM & Stanier RY (1969) Growth and division of some unicellular blue-green algae. J. Gen. Microbiol. 51: 199–202

American Public Health Association (1980) Standard Methods for the Examination of Water and Wastewater, 15th edn. Washington, DC: American Public Association

Bachhuber K & Frösch D (1983) Melamine resins, a new class of water-soluble embedding media for electron-microscopy. J. Microsc. 130: 1–9

Bar-Or Y & Shilo M (1987) Characterization of macromolecular flocculants produced by *Phormidium* sp. strain J-1 and by *Anabaena circularis* PCC 6720. Appl. Environm. Microbiol. 53: 2226–2230

Beveridge, TJ (1981) Ultrastructure, chemistry and function of the bacterial wall. Int. Rev. Cytol. 72: 229–317

Blumenkrantz N & Asboe-Hansen G (1973) New method for quantitative determination of uronic acids. Anal. Biochem. 54: 484–489

Bauer R (1988) Electron spectroscopic imaging: an advanced technique for imaging and analysis in transmission electron microscopy. In: Mayer F (Ed) Methods in Microbiology 20 (pp 113–146). Academic Press, London

Fazio SA, Uhlinger DJ, Parker JH & White DC (1982) Estimations of uronic acids as qualitative measures of extracellular and cell wall polysaccharide polymers from environmental samples. Appl. Env. Microbiol. 43: 1151–1159

Golecki JR (1977) Studies on ultrastructure and composition of cell walls of the cyanobacterium *Anacystis nidulans*. Arch. Microbiol. 141: 35–41

Kallas TJ, Rippka R, Coursin T, Rebrene MC, Demarsac NT & Cohen-Bazire G (1983) Aerobic nitrogen fixation by non-heterocystous cyanobacteria. In: Papageorgiou GC & Packer L (Eds) Photosynthetic Procaryotes: Cell Differentiation and Function (pp 281–302). Elsevier Biomedical, New York

König H (1987) Zellhüllen bei Archaeobakterien, cell envelopes in archaeobacteria. Forum Mikrobiol. 6/87: 209–214

Luft JH (1961) Improvements in epoxy resin embedding methods. J. Biophys. Biochem. Cyt. 9: 409–414

—— (1964) Electron microscopy of cell extraneous coats as revealed by ruthenium red fixative and staining. J. Cell Biol. 23: 54A–55A

Percival E (1979) The polysaccharides of green, red and brown seaweeds: their basic structure, biosynthesis and function. Br. Phycol. J. 14: 103–117

Rees DA (1972) Polysaccharide gels: a molecular view. Chem. Ind. 19: 630–636

Rippka R, Deruelles J, Waterbury JB, Herdman M & Stanier RY (1979) Generic assignments, strain histories and properties of pure cultures of cyanobacteria. J. Gen. Microbiol. 111: 1–61

Sawardeker JS, Sloneker JH & Jeanes A (1965) Quantitative determination of monosaccharides as their alditol acetates by gas-liquid chromatography. Anal. Chem. 37: 1602–1604

Schleifer KH, Steber J & Mayer H (1982) Chemical composition and structure of the cell wall of *Halococcus morrhuae*. Zbl. Bakt. Hyg., I. Abt. Orig. C3: 171–178

Stanier RY & Cohen-Bazire G (1977) Phototrophic procaryotes: the cyanobacteria. Ann. Rev. Microbiol. 831: 225–274

Tease B & Walker RW (1987) Comparative composition of the sheath of the cyanobacterium *Gloeothece* ATCC 27152 cultured with and without combined nitrogen. J. Gen. Microbiol. 133: 3331–3339

Turvey JR (1965) Sulfates of the simple sugars. Adv. Carbohyd. Chem. 20: 183–218

Weckesser J, Broll C, Adhikary SP & Jürgens UJ (1987) 2-*O*-methyl-D-xylose containing sheath in the cyanobacterium *Gloeothece* sp. PCC 6501. Arch. Microbiol. 147: 300–303